Journal of Power Sources 221 (2013) 108–113

Contents lists available at SciVerse ScienceDirect

Journal of Power Sources

journal homepage: www.elsevier.com/locate/jpowsour

The effects of persulfate treatment on the electrochemical properties of $Li[Li_{0.2}Mn_{0.54}Ni_{0.13}Co_{0.13}]O_2$ cathode material

Jun Zheng [a], Shengnan Deng [a], Zhicong Shi [a,c,*], Hongjie Xu [b], Hui Xu [a], Yuanfu Deng [a,c], Zachary Zhang [a,b], Guohua Chen [a,b,*]

[a] Centre for Green Products and Processing Technologies, Guangzhou HKUST Fok Ying Tung Research Institute, Guangzhou 511458, China
[b] Department of Chemical and Biomolecular Engineering, The Hong Kong University of Science and Technology, Clear Water Bay, Kowloon, Hong Kong, China
[c] Key Lab for Fuel Cell Technology of Guangdong Province, Department of Chemistry, School of Chemistry and Chemical Engineering, South China University of Technology, Guangzhou 510640, China

HIGHLIGHTS

- Two kinds of persulfates, $Na_2S_2O_8$ and $(NH_4)_2S_2O_8$, were used to extract excess lithium from $Li[Li_{0.2}Mn_{0.54}Ni_{0.13}Co_{0.13}]O_2$ before charge–discharge test.
- Spherical $Li[Li_{0.2}Mn_{0.54}Ni_{0.13}Co_{0.13}]O_2$ material shows an excellent coulombic efficiency close to 100% at the first cycle after $Na_2S_2O_8$ treatment.
- The enhanced electrochemical performance of the treated $Li[Li_{0.2}Mn_{0.54}Ni_{0.13}Co_{0.13}]O_2$ material is attributed to the extract of excess lithium component and the formation of spinel phase on the surface of the material.

ARTICLE INFO

Article history:
Received 2 May 2012
Received in revised form
20 June 2012
Accepted 21 June 2012
Available online 14 August 2012

Keywords:
Cathode materials
Carbonate precipitate
Persulfate treatment
Rate capability
Lithium-rich compound

ABSTRACT

Spherical $Li[Li_{0.2}Mn_{0.54}Ni_{0.13}Co_{0.13}]O_2$ material was treated with persulfates $Na_2S_2O_8$ or $(NH_4)_2S_2O_8$ to extract lithium to increase the coulombic efficiency of the first cycle. The two persulfates showed different effects. $Na_2S_2O_8$ greatly improved the first cycle efficiency of the active material to nearly 100%. The rate performance was also increased to more than 200 mAh g^{-1} at 1C rate. The reason for the improved rate performance by the treatment of $Na_2S_2O_8$ is attributed to the formation of spinel phase on the surface of the material and the extraction of lithium and oxygen, which results in a decreased electrochemical resistance, whereas the treatment with $(NH_4)_2S_2O_8$ deteriorated the electrochemical performance of the Li-rich compound due to the Li^+/H^+ exchange and the collapse of the layered structure.

1. Introduction

Li-rich compound $xLi_2MnO_3\cdot(1-x)LiMO_2$(M = Mn, Ni, Co, or combinations) has attracted much attention in recent years mainly because of its high capacity of more than 250 mAh g^{-1} at low rate [1–7]. In these compounds, Li_2MnO_3 and Li_2MnO_3-like domains exist with short-range order within a $LiMO_2$ matrix [1]. The Li_2MnO_3 component is proposed and demonstrated to stabilize the crystal structure, resulting in the enhancement of the discharge capacity by simultaneously extracting the lithium with the release of oxygen and a net loss of Li_2O at potential above 4.5 V [7].

One of the drawbacks of these series of materials is that they suffer from a huge irreversible capacity loss of 40–100 mAh g^{-1} in the first cycle depending on their compositions [8]. The irreversible capacity loss is due to the extraction of two lithium ions from Li_2MnO_3 during the charging process and the inability to insert all the lithium ions back into the lattice during the discharge [1,7]. For practical applications of these materials, the first cycle efficiencies must be improved. A strategy to achieve this is to extract certain amounts of lithium from the material prior to the cell assembly using acid treatment. This method can increase the coulombic efficiency to almost 100%. However, this treatment results in the poor cycling stability of the electrode, likely due to the H^+/Li^+ exchange process and the subsequent removal of

* Corresponding authors. Center for Green Products and Processing Technologies, Guangzhou HKUST Fok Ying Tung Research Institute, Guangzhou 511458, China. Tel./fax: +86 20 34685679.
E-mail addresses: zhicong@ust.hk, zcshi@dlut.edu.cnl (Z. Shi), kechengh@ust.hk (G. Chen).

0378-7753/$ – see front matter © 2012 Elsevier B.V. All rights reserved.
http://dx.doi.org/10.1016/j.jpowsour.2012.06.084

oxygen (as H_2O) during the following dehydrating process [9]. Another strategy to make the irreversible capacity loss to 0 mAh g^{-1} is to blend the Li-excessive compounds with Li-free insertion hosts such as V_2O_5, VO_2, LiV_3O_8, $Li_4Mn_5O_{12}$ [8,10,11]. A third strategy to decrease the irreversible capacity loss is that of surface coating, which may be attributed to the retention of some oxide ion vacancies in the lattice after first charge induced surface modification [9]. However, this method cannot eliminate completely the irreversible capacity loss.

The rate capabilities of these materials, with a typical discharge capacity below 200 mAh g^{-1} at 1C, were also dissatisfactory [12]. Al_2O_3 [13], $Al(OH)_3$ [14] or carbon [15] coating can decrease the surface impedance and facilitate the lithium transport through the surface, thus improving the rate performance.

The series of $xLi_2MnO_3\cdot(1-x)LiNi_{1/3}Co_{1/3}Mn_{1/3}O_2$ have been reported to show the best electrochemical performance when $x = 0.5$ [16]. Here we introduce a facile chemical lithium extraction method with the use of oxidizing agents $Na_2S_2O_8$ and $(NH_4)_2S_2O_8$ on the lithium-rich compound to increase the charge–discharge efficiency of the first cycle. The change of the structure and electrochemical properties of $Li[Li_{0.2}Mn_{0.54}Ni_{0.13}Co_{0.13}]O_2$ after treated with the two persulfates were studied. The treatment with $Na_2S_2O_8$ leads to a greatly improved first cycle efficiency and rate performance, with no damage to the cycle stability. While the treatment with $(NH_4)_2S_2O_8$ deteriorated the electrochemical performance of the Li-rich compound due to the Li^+/H^+ exchange and the collapse of the layered structure as seen subsequently.

2. Experimental

2.1. Powder preparation and treatment

The precursor MCO_3 was synthesized using a co-precipitation method. Mn, Ni and Co acetate salt solution with a desired stoichiometric ratio (54:13:13) and Na_2CO_3 solution were added simultaneously to the 60 °C vigorously agitating aqueous solution to form the carbonate precipitate. NH_4OH was added to control the pH of the solution within 7–8. The obtained MCO_3 and Li_2CO_3 (10% excess) were mixed and calcined in air for 5 h at 500 °C and then for 20 h at 900 °C.

The synthesized materials were first blended in $Na_2S_2O_8$ or $(NH_4)_2S_2O_8$ solution. The tested ratios of the persulfate to the active material were 40, 50, and 60% by weight. The mixed solution was stirred and then fully dried. The resulting material was annealed for 10 h to decompose $Na_2S_2O_8$ at 200 °C or $(NH_4)_2S_2O_8$ at 150 °C respectively. Finally, the materials were washed with distilled water three times to remove centrifugally the soluble impurities such as Li_2SO_4 and Na_2SO_4 from the materials. The obtained powders were then dried overnight at 100 °C.

2.2. Structural characterization

X-ray diffraction (XRD) of these samples was performed on a Bruker D8 ADVANCE diffractometer with Cu K α radiation operated at 40 kV and 40 mA. Data were collected in the 2θ range of 10–70° and the patterns were refined by the Rietveld method with the General Structure Analysis Software [17] (GSAS program, Los Alamos National Laboratory, USA). Scanning electron microscopy (SEM) of the samples were observed on a JEOL 6300F electron microscope. X-ray photoelectron spectroscopy (XPS) of the samples were obtained using Kratos Axis Ultra DLD multi-technique surface analysis system, and with monochromatic Al K α radiation, the chemical valence state of the transition metal elements were determined. Binding energies were corrected using C 1s peak (285.0 eV). The surface structure of the active material was studied based on the Raman spectra obtained from a RM3000 spectrophotometer (Renishaw) with a laser wavelength of 632.8 nm and power of 20 mW.

2.3. Electrochemical measurements

Electrochemical measurements were carried out using CR2025 coin cells. The positive electrodes were prepared by coating a slurry containing 80 wt% active materials, 10 wt% Super-P (TIMCAL), 10 wt % PVDF binder (Kynar 761, Arkema Group) on Al current collector foils. Lithium foil and Celgard 2325 (Celgard Inc.) were respectively used as the anode and separator. The electrolyte was 1 M $LiPF_6$ dissolved in DMC/DEC/EC 1:1:1 (volume). The coin cells were assembled in a glove box filled with Argon (Mbruan, Germany). Charge and discharge performances of the cells were investigated using a Neware CT-3008W Tester (Neware Co., Ltd, Shenzhen, China) between 2 and 4.8 V at 25 °C at 1C and 2C rates (1C = 250 mA g^{-1}). EIS of the cells was obtained from a Zahner Zennium electrochemical workstation at the open circuit voltage, with frequencies from 100 KHz to 10 mHz and perturbation amplitude of 10 mV.

3. Results and discussion

SEM of the as-prepared $Li[Li_{0.2}Mn_{0.54}Ni_{0.13}Co_{0.13}]O_2$ (Fig. 1a) shows that most of the particles are spherical. The largest size of the particle is about 10 μm as shown in Fig. 1(b), which is composed of nanoscale primary particles. There are also many smaller particles in the micrometer and sub-micrometer scale dispersed around the larger ones.

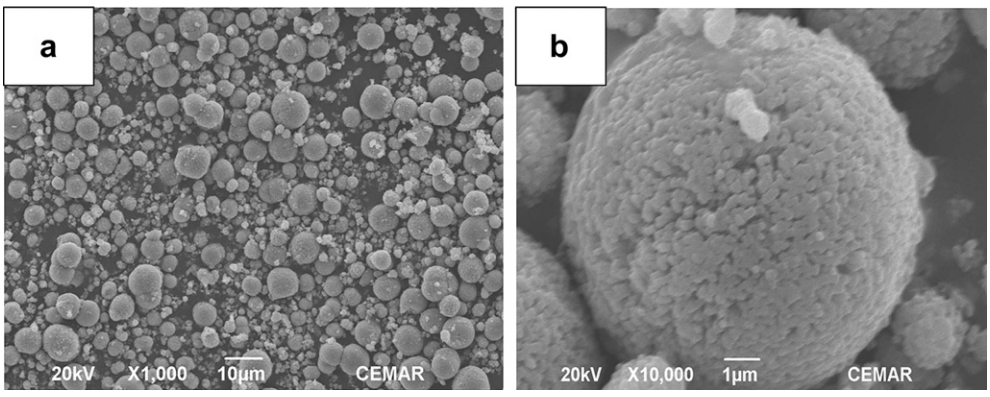

Fig. 1. SEM of as-prepared $Li[Li_{0.2}Mn_{0.54}Ni_{0.13}Co_{0.13}]O_2$ at different magnification.

Fig. 2 shows the XRD pattern and the Rietveld refinement results of GSAS. Because of the complexity of the $xLi_2MnO_3\cdot(1-x)LiMO_2$ structures, the prototypic $R\bar{3}m$ symmetry of layered $LiMO_2$ compounds was used for the refinement [1]. The values of Rp (2.7%), Rwp (3.59%) and χ^2 (1.867) demonstrate a satisfactory refinement. The hexagonal lattice parameter was refined to be $a = 2.844(1)$ Å, $c = 14.218(3)$ Å. The weak reflections within 20° and 25° were originated from the monoclinic Li_2MnO_3-like (C2/m) super lattice, which corresponds to the ordering of the Li^+ and Mn^{4+} ions in the transition metal layer [12].

In order to improve the first cycle efficiency and rate capability, Yu and co-workers of Sanyo Corporation reported a method where surface treatment of the Li-excess material with $(NH_4)_2SO_4$ reagent deintercalates part of lithium ions [12]. When 20 wt% $(NH_4)_2SO_4$ was used, the first cycle efficiency reached 96.5% at 20 mA g^{-1}, as well as a significantly improved rate capability of the cathode materials. The authors attributed the improvement to the modification of the surface into a spinel-like structure as a result of the treatment. On the other hand, oxidizing agent $Na_2S_2O_8$ has been reported to delithiate electrode materials such as $LiCoO_2$ and $LiMn_2O_4$ [18]. Therefore, we introduced two persulfates, $Na_2S_2O_8$ and $(NH_4)_2S_2O_8$, to deintercalate lithium from the lithium-rich compound with intentions to improve the first cycle efficiency and the rate capability.

XRD patterns of $Na_2S_2O_8$ treated samples are shown in Fig. 3. All samples show the overall retention of the layered character with no impurities, indicating no structural change during the treatment. All the byproducts, such as Li_2SO_4 and Na_2SO_4, were washed away during the centrifugation.

The XRD patterns of $(NH_4)_2S_2O_8$ treated samples in Fig. 4 (b, c, and d) show an impurity peak around 19.4°. This is likely due to the slight shift of the (001) peak of Li_2MnO_3 to a higher 2θ value. During the treatment, $(NH_4)_2S_2O_8$ hydrolyzed to NH_4HSO_4, which can in turn decompose to NH_3 and H_2SO_4 under heating. Therefore, the closely packed oxygen planes shear during the Li^+/H^+ ion-exchange reaction to create alternate layers of trigonal prisms where the protons reside, causing a slight contraction of the oxygen layers [19,20]. The intensity ratio of peak (003) to peak (104) is known to be a measure of the cation mixing, and a value smaller than 1.2 is an indication of undesired cation mixing [21]. It can be seen that the intensity ratio of the peak (003) to (104) becomes lower with the amount of $(NH_4)_2S_2O_8$ used. The ratio decreased from 1.38 for pristine material to 1.13 when 60 wt% $(NH_4)_2S_2O_8$ was used, indicating the growth of cation mixing caused by the Li^+/H^+ exchange

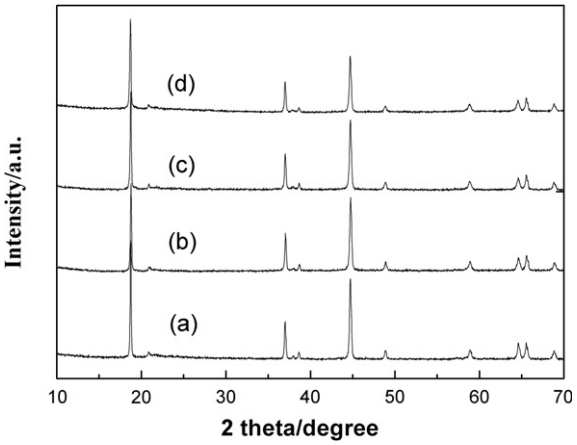

Fig. 3. XRD patterns of $Li[Li_{0.2}Mn_{0.54}Ni_{0.13}Co_{0.13}]O_2$ treated with different amount of $Na_2S_2O_8$ ((a) pristine, (b) 40 wt% (c) 50 wt% (d) 60 wt%).

and the migration of transition metal cations into the lithium layer during the annealing (drying) step of the material [22]. The splitted peaks of (006) and (102) indicate that $LiMO_2$ has a layered structure. After the treatment, one can see that the resolved doublet peaks (006) and (102) gradually merge into a single broad peak. This suggests that the layered structure is destroyed, which may damage the electrochemical performance of $Li[Li_{0.2}Mn_{0.54-}Ni_{0.13}Co_{0.13}]O_2$ as seen subsequently.

Fig. 5 shows the 1st and 2nd cycle charge–discharge profiles of $Li[Li_{0.2}Mn_{0.54}Ni_{0.13}Co_{0.13}]O_2$ after the treatment with $Na_2S_2O_8$ at 1C (250 mA g^{-1}). The charge profile exhibits two phases. The one below 4.5 V is associated with the oxidation of Ni^{2+} to Ni^{4+} and Co^{3+} to Co^{4+} [16]. The other at approximately 4.5 V becomes smaller with the amount of $Na_2S_2O_8$ used due to the loss of oxygen from the layered Li_2MnO_3 lattice [23,24]. This shows that the extraction extent of lithium increases the first cycle efficiency of the compounds. When 40, 50 and 60 wt% $Na_2S_2O_8$ were applied, the efficiencies were 78.85 and 85.04 and 98.7%, respectively, much higher than that of the pristine material, which is about 55.85%. Chemical extraction of lithium before the electrochemical tests can reduce the first-cycle irreversible capacity loss to near 0 mAh g^{-1} without compromising the discharge capacity.

Fig. 6 indicates that increasing the amount of $Na_2S_2O_8$ also enhances the capacity of $Li[Li_{0.2}Mn_{0.54}Ni_{0.13}Co_{0.13}]O_2$ at 1C and 2C

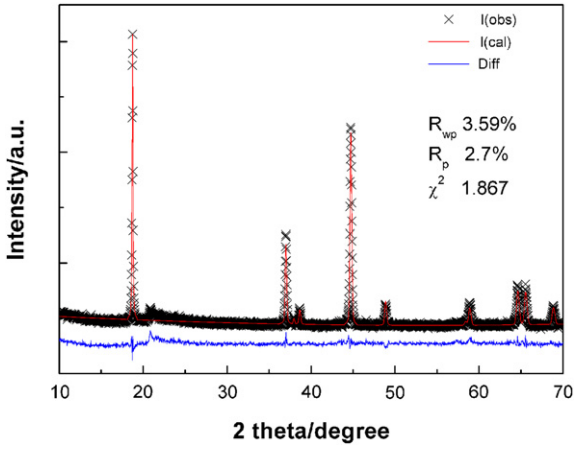

Fig. 2. Rietveld refined results for the XRD pattern of $Li[Li_{0.2}Mn_{0.54}Ni_{0.13}Co_{0.13}]O_2$ material.

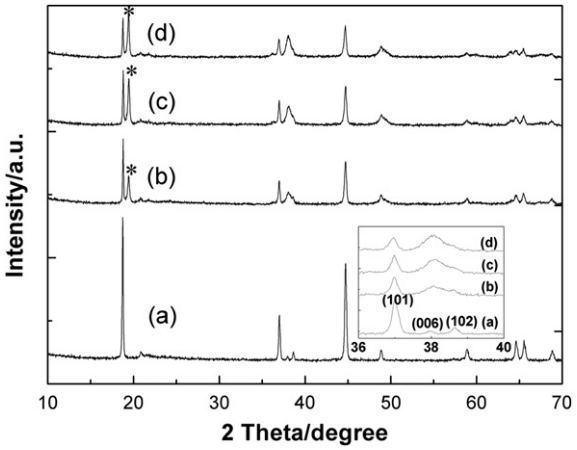

Fig. 4. XRD patterns of $Li[Li_{0.2}Mn_{0.54}Ni_{0.13}Co_{0.13}]O_2$ treated with different amount of $(NH_4)_2S_2O_8$ ((a) pristine, (b) 40 wt% (c) 50 wt% (d) 60 wt%).

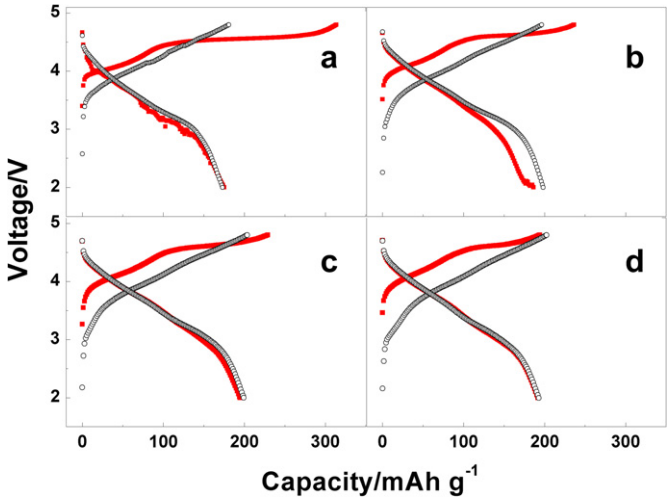

Fig. 5. The 1st (solid square) and 2nd (hollow circle) charge–discharge curves of Li[$Li_{0.2}Mn_{0.54}Ni_{0.13}Co_{0.13}$]$O_2$ at 1C treated with different amount of $Na_2S_2O_8$ ((a) pristine, (b) 40 wt% (c) 50 wt% (d) 60 wt%).

rates. The detailed electrochemical data are listed in Table 1. The cells endured an activation process where the capacity gradually increased in the initial 20 cycles. At the 1st and 50th cycles, the specific discharge capacity of the treated samples was 191.6 and 181.9 mAh g^{-1}, respectively. This is significantly higher than the specific discharge capacity of the 1st and 50th cycles of the pristine material, which was 175.2 and 152.1 mAh g^{-1}, respectively. The capacity retentions of the samples were similar with values being all above 80% as shown in Table 1, indicating that the retention of the capability does not change significantly with the use of $Na_2S_2O_8$ at 1C. Although the capacity retentions of the treated materials at 2C rates were slightly lower, they were still higher than those of the reported $(NH_4)_2SO_4$-treated samples, which only delivered 62% specific capacity of the initial one after 30 cycles [12].

The charge–discharge profiles of Li[$Li_{0.2}Mn_{0.54}Ni_{0.13}Co_{0.13}$]$O_2$ treated with $(NH_4)_2S_2O_8$ show that the 1st charge–discharge cycle efficiency was also enhanced (Fig. 7), although the capacity was lower than that of the pristine one. When the amount of $(NH_4)_2S_2O_8$ reached 60 wt%, the treated cathode material showed higher discharge capacity than charge capacity, indicating that too many lithium ions had been extracted during the treatment.

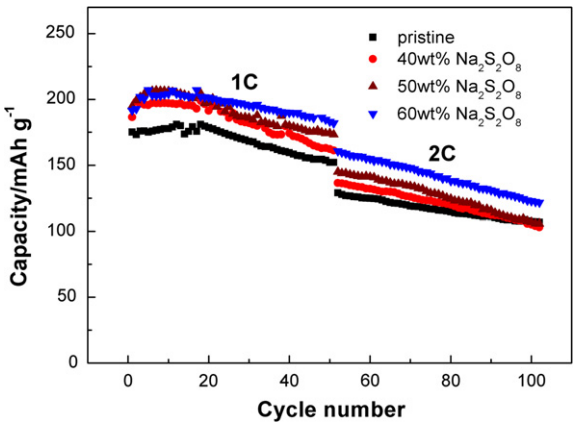

Fig. 6. Cycle performance of Li[$Li_{0.2}Mn_{0.54}Ni_{0.13}Co_{0.13}$]$O_2$ treated with $Na_2S_2O_8$ solution at 1C and 2C rates.

Table 1
Electrochemical properties of Li[$Li_{0.2}Mn_{0.54}Ni_{0.13}Co_{0.13}$]$O_2$ treated with $Na_2S_2O_8$.

Amount of $Na_2S_2O_8$	1st cycle capacity (mAh g^{-1})	The highest capacity (mAh g^{-1})	50th cycle capacity (mAh g^{-1})	50 Cycle retention at 1C	50 Cycle retention at 2C
Pristine	175.2	181.1	152.1	84.0%	82.7%
40 wt%	186.5	198.9	161.2	81.1%	75.6%
50 wt%	194.8	206.1	173.3	83.8%	73.0%
60 wt%	191.6	207.1	181.9	87.8%	75.7%

Fig. 8 compares the cycle capability at 1C and 2C rates of $(NH_4)_2S_2O_8$ treated samples. Although there was a significant capacity increase during the activation process, the capacity of the samples was still not satisfactory. The highest capacity is less than 140 mAh g^{-1} when 40 wt% $(NH_4)_2S_2O_8$ was used, much lower than that of the samples treated with $Na_2S_2O_8$. Furthermore, increasing the amount of $(NH_4)_2S_2O_8$ deteriorates the electrochemical performance. The electrochemical data clearly demonstrate that the Li-rich compounds were damaged by the $(NH_4)_2S_2O_8$ treatment.

The reason for the poor electrochemical performance of $(NH_4)_2S_2O_8$ treated samples compared with $Na_2S_2O_8$ may be attributed to the pH variation of the solution during the treatment process caused by chemical decomposition. The pH values of 40, 50, and 60 wt% $(NH_4)_2S_2O_8$ solution with Li[$Li_{0.2}Mn_{0.54}Ni_{0.13}Co_{0.13}$]$O_2$ after stirring were 7.4, 7.3, and 7.1, respectively, while the same weight percentages for the $Na_2S_2O_8$ solution after the treating process had pH values of 9.1, 8.7, and 8.3, respectively. However, when the solution that containing $(NH_4)_2S_2O_8$ was heated to evaporate water, the pH value dropped quickly to around 2, while the pH value of the solution containing $Na_2S_2O_8$ was still higher than 7 after heating for 30 min, and higher than 6 even when water was almost dried up. The low pH value of the heated $(NH_4)_2S_2O_8$ solution was likely resulted from the decomposition of NH_4HSO_4 to NH_3 and H_2SO_4. The emergence of strong acid H_2SO_4 makes the Li^+/H^+ exchange so fast that it damaged the layered structure of Li[$Li_{0.2}Mn_{0.54}Ni_{0.13}Co_{0.13}$]$O_2$. On the other hand, $Na_2S_2O_8$ was more stable than $(NH_4)_2S_2O_8$ in the solution during heating, which only

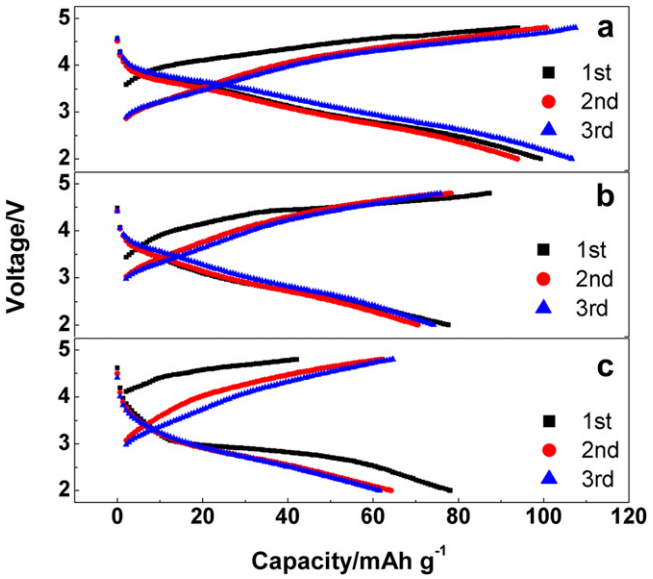

Fig. 7. The 1st (square), 2nd (circle) and 3rd (triangle) charge–discharge curves of Li[$Li_{0.2}Mn_{0.54}Ni_{0.13}Co_{0.13}$]$O_2$ at 1C treated by different concentration of $(NH_4)_2S_2O_8$ solution ((a) 40 wt% (b) 50 wt% (c) 60 wt%).

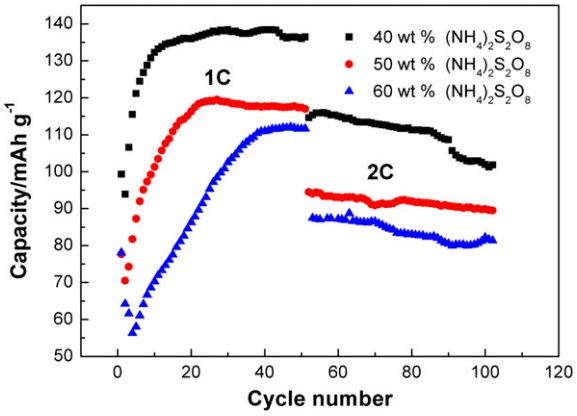

Fig. 8. Cycle performance of $Li[Li_{0.2}Mn_{0.54}Ni_{0.13}Co_{0.13}]O_2$ treated with $(NH_4)_2S_2O_8$ at 1C and 2C rates.

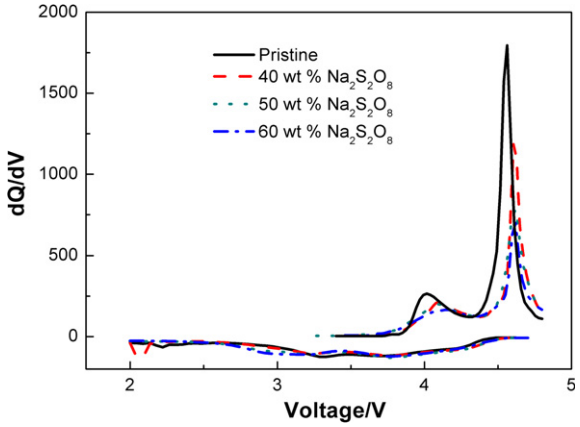

Fig. 10. dQ/dV plots of the 1st cycle for treated $Li[Li_{0.2}Mn_{0.54}Ni_{0.13}Co_{0.13}]O_2$.

results in a minor change of pH value. That is likely to be the reason why the electrochemical performance of $Li[Li_{0.2}Mn_{0.54}Ni_{0.13}Co_{0.13}]O_2$ treated with $Na_2S_2O_8$ was better than that of the ones treated with $(NH_4)_2S_2O_8$.

The dashed lines in Fig. 9 indicate that after the treatment of $Na_2S_2O_8$, Ni^{2+}, Co^{3+}, Mn^{4+} $2P_{3/2}$ remain at their original binding energies of 642.4, 780.5, and 855.1 eV, respectively. Therefore, the valences of Mn, Co, Ni did not change after the precondition process. Since lithium was extracted from the active material during the process, some oxygen might be released from the lattice in order to keep the valences balanced. The differential capacity dQ/dV plots also support this suggestion. Comparing the four voltage profiles in Fig. 10, the major difference lies in the peak in the region of 4.5–4.6 V, which corresponds to the release of O_2 from the active material. The obvious decrease in the intensity and the area of the peak with the increase of $Na_2S_2O_8$, implies that the O_2 release was greatly suppressed after the treatment. This suggests that a certain amount of oxygen ions may have been leached together with lithium ions from the lattice of the active material during the $Na_2S_2O_8$ treatment.

The reaction mechanism may be as follows:

$$Li_{1.2}M_{0.8}O_2 + xNa_2S_2O_8 \rightarrow Li_{1.2-2x}M_{0.8}O_{2-x} + xNa_2SO_4 + xLi_2SO_4 + x/2O_2$$

Raman spectroscopy was obtained to investigate the change in the surface structure of $Li[Li_{0.2}Mn_{0.54}Ni_{0.13}Co_{0.13}]O_2$. In Fig. 11, the pristine material shows two major peaks at around 480 and 596 cm^{-1}, which correspond to the M–O stretching ν_1 (A_{1g}) and the O–M–O bending ν_2 (E_g) of layered $LiMO_2$ compound, respectively. After the $Na_2S_2O_8$ treatment, the 596 cm^{-1} peak disappeared and a new peak at 620–632 cm^{-1} emerged, which indicates that there was a change of the surface structure of the active material. These new peaks resemble those of spinel material. The peak at 625 cm^{-1} (A_{1g}) represents the Mn–O symmetrical vibration in MnO_6 octahedron, whereas the peak at 480–485 cm^{-1} corresponds to one of T_{2g} symmetries of the spinel material [25].

Yu and co-workers reported that the $(NH_4)_2SO_4$ treatment on $Li_{1.2}M_{0.8}O_2$ leads to the formation of spinel-like structure [12]. Since spinel is structurally compatible with the layered structure, where both share the same oxygen arrangement but differ in their arrangements of Li and transition-metal atoms, the formation of a surface spinel layer most likely involves the removal of Li and O from the surface of Li-excess materials. Therefore, the major reason

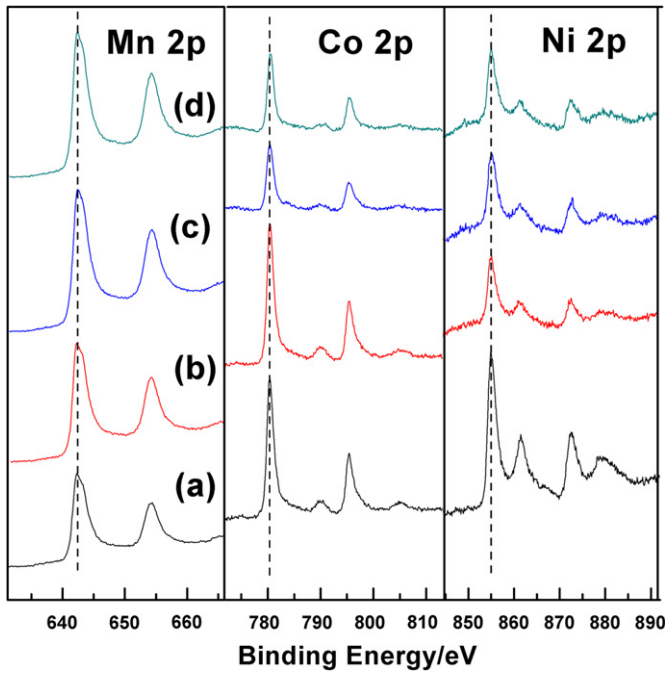

Fig. 9. XPS spectra of Mn 2p, Ni 2p and Co 2p in $Li[Li_{0.2}Mn_{0.54}Ni_{0.13}Co_{0.13}]O_2$ treated with different amount of $Na_2S_2O_8$((a) pristine, (b) 40 wt% (c) 50 wt% (d) 60 wt%).

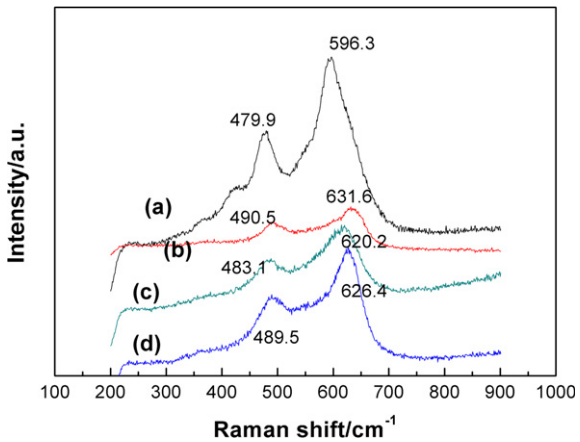

Fig. 11. Raman spectra of $Li[Li_{0.2}Mn_{0.54}Ni_{0.13}Co_{0.13}]O_2$ treated with different amount of $Na_2S_2O_8$ ((a) pristine, (b) 40 wt% (c) 50 wt% (d) 60 wt%).

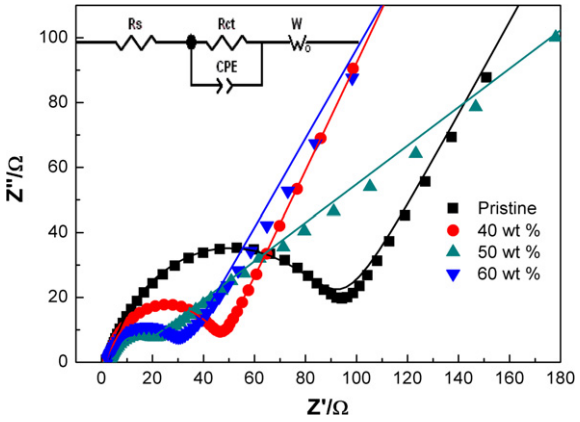

Fig. 12. EIS plots of the $Li[Li_{0.2}Mn_{0.54}Ni_{0.13}Co_{0.13}]O_2$ treated with $Na_2S_2O_8$. The inset shows the equivalent circuit for the impedance spectra. The lines in the plots represent fitting results.

for the improved rate capabilities of $Na_2S_2O_8$ treated samples is likely due to the formation of the spinel-like phase on the surface of pristine $Li[Li_{0.2}Mn_{0.54}Ni_{0.13}Co_{0.13}]O_2$.

The EIS measurements of the pristine and treated samples were carried out at open circuit status. All impedance spectra curves in Fig. 12 are composed of a depressed semicircle in high frequency region and a sloping line in low frequency region, each corresponding to the charge transfer process and the lithium ion diffusion in the bulk of the material, respectively. An equivalent circuit model was found (Fig. 12 inset) to fit the impedance spectra well; where R_s is the resistance of the solution and R_{ct} is the charge transfer resistance in the electrode/electrolyte interface. Constant phase-angle element (CPE) indicates the non-ideal double layer capacitance, where W_o refers to Warburg impedance. The fitted results of EIS are consistent with electrochemical properties of the pristine and treated lithium rich compounds. There was a huge reduction in the resistance of charge transfer, from 85.39 Ω of composite electrode fabricated based on pristine $Li[Li_{0.2}Mn_{0.54}Ni_{0.13}Co_{0.13}]O_2$ to less than 50 Ω when the same electrode material is treated with $Na_2S_2O_8$. The reduction of R_{ct} may facilitate lithium transfer on the electrode/electrolyte interface, thus leads to improved rate capability. The decreased slope in the low frequency region for 50wt% sample requires further analysis which is beyond the scope of this study.

4. Conclusion

The layered solid solution $Li[Li_{0.2}Mn_{0.54}Ni_{0.13}Co_{0.13}]O_2$ had been synthesized and treated with either $Na_2S_2O_8$ or $(NH_4)_2S_2O_8$. The use of $Na_2S_2O_8$ improved the first cycle charge–discharge efficiency of the active material to nearly 100%, in addition to enhanced rate performance. The $(NH_4)_2S_2O_8$ treated samples showed poor electrochemical performance due to structure damages at low pH. A reaction mechanism for the $Na_2S_2O_8$ treatment is proposed, in which lithium and oxygen are extracted simultaneously from the active material and the transitional metal elements retain the same valence. Raman spectra indicated the formation of spinel phase on the surface of the active material. This spinel phase with a three-dimensional diffusion route can decrease the charge transfer resistance as well as facilitate the lithium ion transfer and diffusion process through the surface, leading to an improved electrochemical performance.

Acknowledgments

This work is supported by the National Natural Science Foundation of China (Grant No. 21176045), the Specialized Research Fund for the Doctoral Program of Higher Education of China (20090041120020), the Fundamental Research Funds for the Central Universities (SCUT2012ZZ0042), the Guangdong Province Sci & Tech Bureau (Grant No. 2010B091000004, No. 2011B05030008), and the Fok Ying Tung Foundation (NRC07/08.EG01).

References

[1] S.H. Kang, C.S. Johnson, J.T. Vaughey, K. Amine, M.M. Thackeray, J. Electrochem. Soc. 153 (2006) A1186–A1192.
[2] M.M. Thackeray, C.S. Johnson, J.T. Vaughey, N. Li, S.A. Hackney, J. Mater. Chem. 15 (2005) 2257–2267.
[3] M.M. Thackeray, S.H. Kang, C.S. Johnson, J.T. Vaughey, R. Benedek, S.A. Hackney, J. Mater. Chem. 17 (2007) 3112–3125.
[4] K. Numata, S. Yamanaka, Solid State Ionics 118 (1999) 117–120.
[5] A. Ito, D. Li, Y. Sato, M. Arao, M. Watanabe, M. Hatano, H. Horie, Y. Ohsawa, J. Power Sources 195 (2010) 567–573.
[6] J.H. Lim, H. Bang, K.S. Lee, K. Amine, Y.K. Sun, J. Power Sources 189 (2009) 571–575.
[7] J.M. Zheng, Z.R. Zhang, X.B. Wu, Z.X. Dong, Z. Zhu, Y. Yang, J. Electrochem. Soc. 155 (2008) A775–A782.
[8] J. Gao, J. Kim, A. Manthiram, Electrochem. Commun. 11 (2009) 84–86.
[9] Y. Wu, A.V. Murugan, A. Manthiram, J. Electrochem. Soc. 155 (2008) A635–A641.
[10] E.S. Lee, A. Manthiram, J. Electrochem. Soc. 158 (2001) A47–A50.
[11] J. Gao, A. Manthiram, J. Power Sources 191 (2009) 644–647.
[12] D.Y.W. Yu, K. Yanagida, H. Nakamura, J. Electrochem. Soc. 157 (2010) A1177–A1182.
[13] Y. Wu, A. Manthiram, Electrochem. Solid State Lett. 9 (2006) A221–A224.
[14] Y.J. Kang, J.H. Kim, S.W. Lee, Y.K. Sun, Electrochim. Acta 50 (2005) 4784–4791.
[15] J. Liu, Q. Wang, B. Reeja-Jayan, A. Manthiram, Electrochem. Commun. 12 (2010) 750–753.
[16] X. J Guo, Y. X Li, M. Zheng, J.M. Zheng, J. Li, Z.L. Gong, Y. Yang, J. Power Sources 184 (2008) 414–419.
[17] A.C. Larson, R.B. Von Dreele, "General Structure Analysis System (GSAS)" Los Alamos National Laboratory Report LAUR 86-748 (2000).
[18] S.J. Yan, M.G. Zhang, Y.M. Tian, G. Sun, W.H. Tian, Chin. J. Inorg. Chem. 25 (2009) 491–495.
[19] Y. Paik, C.P. Grey, C.S. Johnson, J.S. Kim, M.M. Thackeray, Chem. Mater. 14 (2002) 5109–5115.
[20] C.S. Johnson, J.S. Kim, C. Lefief, N. Li, J.T. Vaughey, M.M. Thackeray, Electrochem. Commun. 6 (2004) 1085–1091.
[21] K.M. Shaju, G.V. Subba Rao, B.V.R. Chowdari, Electrochim. Acta 48 (2002) 145–151.
[22] C.S. Johnson, N. Li, C. Lefief, J.T. Vaughey, M.M. Thackeray, Chem. Mater. 20 (2008) 6095–6106.
[23] Z. Lu, L.Y. Beaulieu, R.A. Donaberger, C.L. Thomas, J.R. Dahn, J. Electrochem. Soc. 149 (2002) A778–A791.
[24] A.R. Armstrong, M. Holzapfel, P. Novak, C.S. Johnson, S.H. Kang, M.M. Thackeray, P.G. Bruce, J. Am. Chem. Soc. 128 (2006) 8694–8698.
[25] R. Baddour-Hadjean, J. Pereira-Ramos, Chem. Rev. 110 (2010) 1278–1319.